

Microstructure and surface degradation of Al reinforced by Al_xW intermetallic compounds via different fabrication routes

Angeliki G. Lekatou^{1,*}, Maria Mpalanou¹, Konstantinos Lentzaris¹, Alexander E. Karantzalis¹ and Nikolaos Melanitis²

¹ Laboratory of Applied Metallurgy, Department of Materials Engineering, University of Ioannina, 45110 Ioannina, Greece

² Applied Engineering and Marine Materials Sector, Hellenic Naval Academy, 18539 Piraeus, Greece

Abstract. In the present effort, Al- Al_xW composites have been prepared by vacuum arc melting (VAM), conventional casting (CAST) and free sintering (PM) with the objective to determine an effective fabrication route in terms of low cost, ease of manufacture and property boosting. The produced Aluminium Matrix Composites (AMCs) contain several types of in-situ aluminides. Their morphology, stoichiometry and distribution strongly depend on the fabrication route. The particulate aluminide reinforcements have a beneficial effect on the wear response of the monolithic matrix. VAM-AMCs show the highest resistance to wear. A wear mechanism is proposed.

1 Introduction

Reinforcement of aluminium with particles of Al-based intermetallic compounds (IMCps) has led to notably improved properties of Al, such as mechanical properties [1-5], corrosion and wear resistance [6-11]. Particulate IMC reinforcement of Al can be attained by ex-situ introduction of the IMCps into the Al-matrix or by in-situ processing of the Al-matrix with the IMC constituent elements. In-situ processing can be realized by various methods, like liquid metal infiltration, powder metallurgy, various casting techniques and mechanical alloying [5].

Amongst the IMCs, the aluminides of transition metals have received great attention, since they combine good high temperature mechanical properties, light weight, high melting points, high corrosion and wear resistance [12]. The majority of the investigations on the alloy design and properties concern the aluminides of Ni, Fe and Ti. Research on the aluminides of refractory metals (RM) is quite limited possibly due to the high costs and the low workability of the RMs. However, an RM, such as W, has excellent properties. For example, just a small amount of a heavy refractory powder as reinforcement is enough to lead to notable mechanical property improvements [13]. In-situ formed tungsten aluminides have been shown to be the main reason for the significant increase in the sliding wear

* Corresponding author: alekatou@cc.uoi.gr

resistance of Al/WCp composites [7,10]; their beneficial contribution into the corrosion resistance to acid rain and saline environments has also been manifested [7,11]. Laser surface alloying of Al with W, resulting in the formation of Al₄W, W and Al led to a substantial enhancement of the corrosion resistance [14]. The above findings provide a strong motive to investigate the ability to prepare Al reinforced by tungsten aluminides by simple and relatively low-cost methods.

Several works have brought out the beneficial effect of in-situ IMC particulate reinforcements of Al, such as Al₃Ti [15], (Al₂O₃ + Ti(Al_{1-x},Fe_x)₃) [16], TiB₂ [17], AlB₂ [18], (Al₁₂W+Al₅W+Al₃(Ti,W)) [7], Al₃Zr [19], ZrB₂ [20], (ZrB₂+TiB₂) [21], Al₉Co₂ [9], on the wear resistance of Al. The formation of strong interfacial bonds between the IMC and Al is reported as the main reason for such improvements [22].

Considering the brittleness-due difficulties in manufacturing monolithic Al-W IMCs, the present effort focuses on the fabrication of composite microstructures, toughened by IMC reinforcements. This preliminary study especially deals with: (a) investigating an effective fabrication route with respect to cost, ease of manufacture and property enhancement by adopting three manufacturing methods, and (b) assessing the sliding wear performances of the produced materials and their relationship with the preparation method.

2 Experimental procedure

Aluminium Matrix Composites (AMCs) were produced via vacuum arc re-melting (VAM, ×3), stir casting (CAST) and free sintering (PM). VAM-AMCs were prepared by introducing a mixture of Al granules (99.7% pure, <1 mm) and W powder (99.9% pure, <12 μm) into the water-cooled copper crucible of the arc furnace. Further details are reported in [8]. CAST-AMCs were prepared by adding appropriate amounts of Al₄W (produced by VAM followed by mechanical milling) and K₂TiF₆ wetting agent in an Al1050 melt (830 °C). Further details can be found in [7]. In the case of PM-AMCs, the same (as in VAM) mixture of Al and W, was pressed at 25 MPa and then heated for 2 h at 650 °C under argon. Briquettes of 15 mm diameter and 4 mm height were produced.

The microstructure inspection of polished specimens was conducted by SEM/EDX (JEOL JSM 6510 LV / Oxford Instruments X-Act EDS) under Secondary Electron (SE) and Backscattering Electron Composition (BEC) modes. X-ray Diffraction (XRD) was carried out by the Bruker D8 Advance Diffractometer. The quantitative phase composition and the 2D-porosity of the alloys were estimated by image analysis (Image J software). The specimen hardness (in cross-section) was measured by the Innovatest IN-700M tester. Dry sliding wear experiments were performed at a CSM ball-on-disc tribometer (normal load: 1N, sliding speed: 10 cm/s, sliding distance: 1000 m, counter-body: AISI-52100 steel ball).

3 Results and Discussion

3.1 Microstructural observations

The interpretation of the microstructure utilizes the Al-Ti, Al-W and Ti-W phase diagrams [23]. Fig. 1 presents the microstructures of the AMCs and the corresponding XRD patterns. Table 1 presents the calculated, through image analysis, 2D porosity, 2D coverage area by the IMCs and the hardness of the AMCs. The following considerations attempt to clarify the findings of Fig. 1 and Table 1:

Regarding the VAM-AMC, the employed Al-W composition corresponds to the αAl+Al₁₂W stability area of the Al-W system under equilibrium. During solidification, W is engaged in the aluminide lattice that is solidified first, namely Al₄W. Al₄W has the lowest

enthalpy of formation amongst all Al-W IMCs [24]; its predominance in the final material is, thereby, justified. The high cooling rates during solidification following arc melting, have not allowed for completion of the diffusion processes; hence, the peritectic reactions predicted from the equilibrium Al-W phase diagram [23]:



have partially (reaction 1) or totally (reaction 2) been suppressed. Consequently, Al_4W (primarily) and Al_5W are the IMC phases formed, as determined by XRD and EDX. Fig. 1 manifests a more homogeneous phase distribution in the VAM-AMC, as compared to the CAST and PM AMCs, realized by the ($\times 3$) remelting along with the high diffusion rates (temperatures of the order of 2000-2500°C and liquid state diffusion).

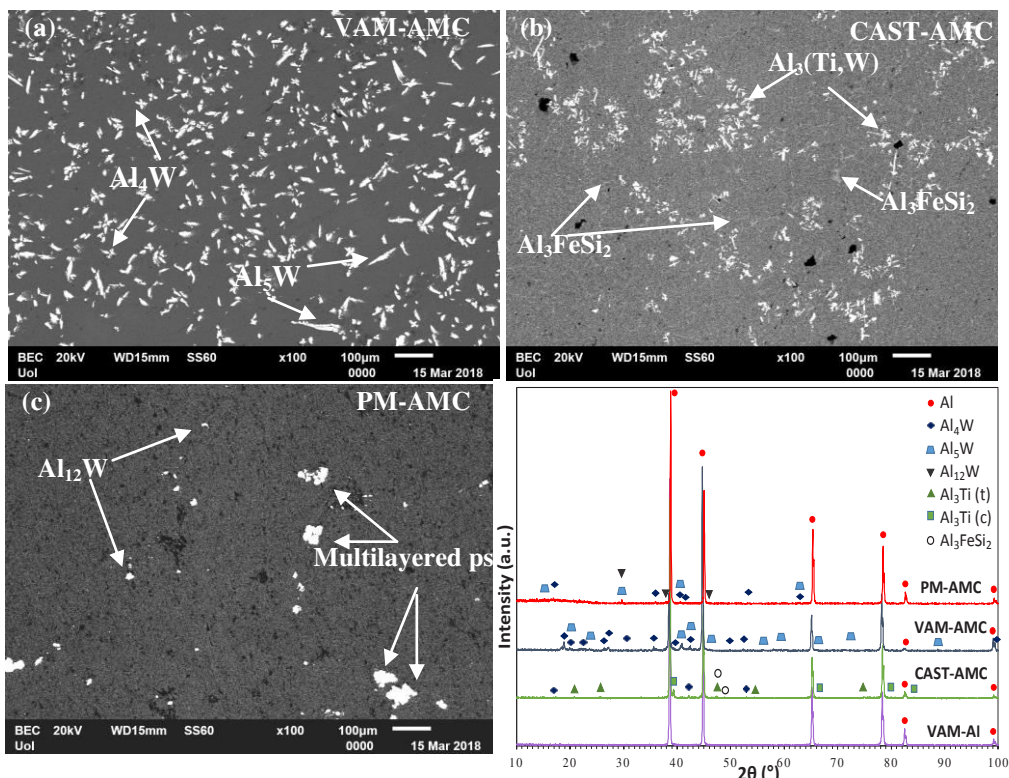


Fig. 1. (a-c) BEC micrographs of the AMCs prepared by: (a) vacuum arc melting, (b) casting, (c) powder metallurgy; (d) XRD patterns of the AMCs and monolithic Al; (t): tetragonal, (c): cubic

Table 1. Microstructural and hardness data of the examined AMCs

	Initial composition (wt.%)	2D Porosity (%)*	2D IMC coverage area (%)*	Hardness (HB ₁₀)
VAM-AMC	Al-5W	0.66	12.97 (Al ₄ W+Al ₅ W)	49.05 ± 3.7
CAST-AMC	Al-2.0W-1.1Ti	1.05	5.50 (Al ₃ (Ti,W)+minorAl ₄ W)	46.58 ± 4.9
PM-AMC	Al-5W	3.29	1.76 (Al ₁₂ W+Al ₄ W + Al ₅ W)	40.67 ± 6.5

*AMCs presented in Fig. 1

Regarding the CAST-AMC, the main IMC formed is Al_3Ti , according to [25]:



W is mostly found in solid solution with Ti within the Al_3Ti structure ($Al_3(Ti,W)$) in quantities less than 1 at% W. Occasionally, submicron particles of $Al_{4-x}W$ are observed in segregates of Al-Ti-W (Fig. 2). The above observations indicate that Al_4W has partly reacted with K_2TiF_6 forming $Al_3(Ti,W)$. It should also be noted that Al_3Ti has higher stability than Al_4W , as the enthalpy of Al_3Ti formation (-40350 kJ/mol [26]) is much lower than the enthalpy of formation of Al_4W (~-11200 kJ/mol) [24].

The inclusion of W in the Al_3Ti structure may be justified by the formation of solid solutions between Ti and W in a wide range of stoichiometries at the holding temperature [23]. It is herein postulated that during casting and solidification, a quantity of W has remained trapped in the Al_3Ti lattice leading to a metastable $Al_3(Ti,W)$ structure. Jahnatek et al [27] reported that alloying of tetragonal Al_3Ti with transition metals having more d-electrons in their valence band (case of W) can result in the transformation of the stable D022 tetragonal lattice to the metastable L12 cubic lattice. Detection of accountable amounts of cubic Al_3Ti (Fig.1d) in the CAST-AMC supports the above postulation. A small but accountable segregation despite rigorous stirring could not be avoided (Fig. 2), as the specific weight of Al_4W (6.04 g/cm³) [28], is higher than that of Al_3Ti (3.36 g/cm³) [29] and, especially, Al (2.7 g/cm³).

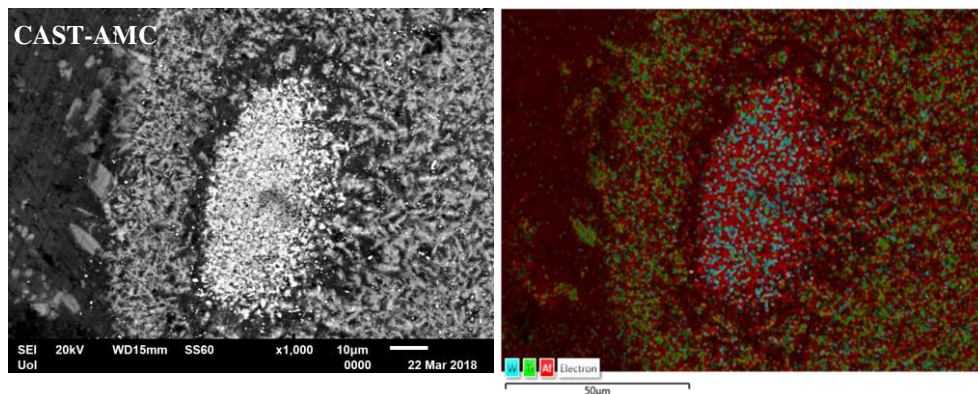


Fig. 2. SE micrograph of CAST-AMC showing segregation of Al_4W and $Al_3(Ti,W)$ and respective EDX map (light-blue: W, green: Ti, red: Al)

Regarding PM-AMC, free sintering led to the formation of coarse multi-layered agglomerates of Al-W IMCps of variable sizes within Al. Some of them present cores of W (Fig. 3, Sp.1). This arrangement can be justified as follows: As the W solubility limit in αAl is very low, sintering favors the immediate precipitation of Al-W IMCs. The larger diffusion coefficient of Al in W than W in Al allows Al atoms to diffuse toward W atoms, leading to the immediate formation of the intermetallic compound that is the richest in Al; namely $Al_{12}W$. As soon as the available W is consumed in the formation of IMCs, sintering of neighboring Al occurs, resulting in the envelopment of the IMCps by the Al-matrix.

The multilayered structure of the IMC micro-constituents along with the detection of a variety of W-aluminides (besides $Al_{12}W$, Al_4W and Al_5W identified by XRD and EDX, EDX showed the presence of $Al_{77}W_{23}$, as well) can be justified by the nature of the free sintering process and the precursor powders. Under the applied sintering conditions, the involved reactions between Al and W are diffusion driven solid state reactions. Bi-atomic exchanges between the powder particles, as diffusion advances, can give various stoichiometries and concentrations eventually covering nearly the whole range of phases predicted by the Al-W phase diagram [6]. The multilayer growth mechanism is often observed in solid state diffusion processes [5]. Moreover, the presence of porosity (Table 1)

and oxidation products in the PM-AMC are typical drawbacks of the powder metallurgical procedures. Porosity is mostly ascribed to the well-known Kirkendall effect [30,31].

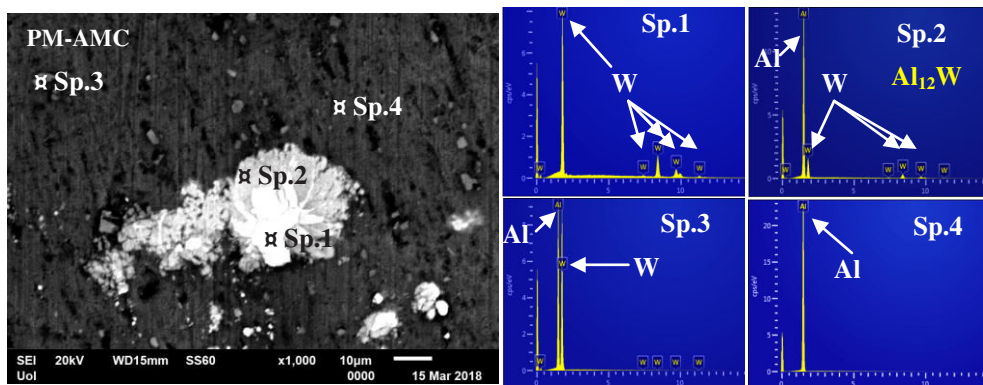


Fig. 3. SE micrograph of PM-AMC and representative point EDX spectra

Besides coarse multilayered particles, Fig.1c shows dispersion of fine (often sub-micron) particles. Fig.3, Sp.2 suggests that these fine particles stem from the disintegration (and migration of the finest ones) of the outer intermetallic layers. The disintegration of IMCps can be attributed to the Kirkendall effect [32]. The counter-diffusion causes the formation of several vacancies accompanied by volume expansion. Thereby, tensile stresses are exerted in the outer layers of the IMC particles, whilst compressive stresses are exerted in the interior of the particles. This can lead to the formation of micro-cracks in the brittle intermetallics and eventually fragmentation of their outer parts [33].

3.2 Sliding wear behaviour

Fig.4(a-d) presents the wear track morphology and the wear rates (w.r.) of the AMCs. Fig. 4(d) manifests the beneficial action of the IMCps in the wear rate reduction. The higher wear resistance of the AMCs compared to monolithic Al (CAST-Al w.r.>CAST-AMC w.r., VAM-Al w.r.>VAM-AMC w.r.) is mainly attributed to the following: (i) coarse IMCps reduce the load transferred to the matrix; (ii) fine IMCps (PM-AMC case) act as matrix strengthening elements rather than load-sharing ones; (iii) the dispersed phases reduce the direct contact area between matrix and counter-face; (iv) IMCps provide thermal stability to the matrix; [7,9,10,15,19,34,35]. In all cases, the periodic «hill-valley» morphology [36] is observed, suggesting that the metallic nature of the AMCs has been maintained. Such a landscape formation has previously been analysed in terms of intensive plastic deformation of the soft matrix in front of the counter-body steel ball causing notable material flow at directions, parallel and perpendicular to the sliding direction [7,9,10,34,37].

The lowest wear rate of VAM-AMC is associated with the most uniform dispersion of IMCs (Fig.1a) being responsible for the smoothest wear surface (Fig.4a), the highest hardness, the lowest porosity and the lowest surface area of Al (Table 1). The highest wear rate of PM-AMC is associated with the highest porosity, the highest plastic deformation due to the highest surface area of Al and the lowest hardness (Table 1). Analogous concept justifies the intermediate wear rate of CAST-AMC (Fig. 4d). The intergranular presence of the brittle eutectic Al₃FeSi₂ in CAST-AMC (Fig. 1b,d) increases the probability for cracking initiation/growth. It should be noted that although PM-AMC presents three times higher porosity than CAST-AMC, its wear rate is slightly lower than that of CAST-AMC and within experimental error. (Porosity degrades wear behaviour, due to the reduction of

the carrying load solid area [38]. The main reason for such discrepancy is postulated to be the high dispersion of very fine IMC fragments.

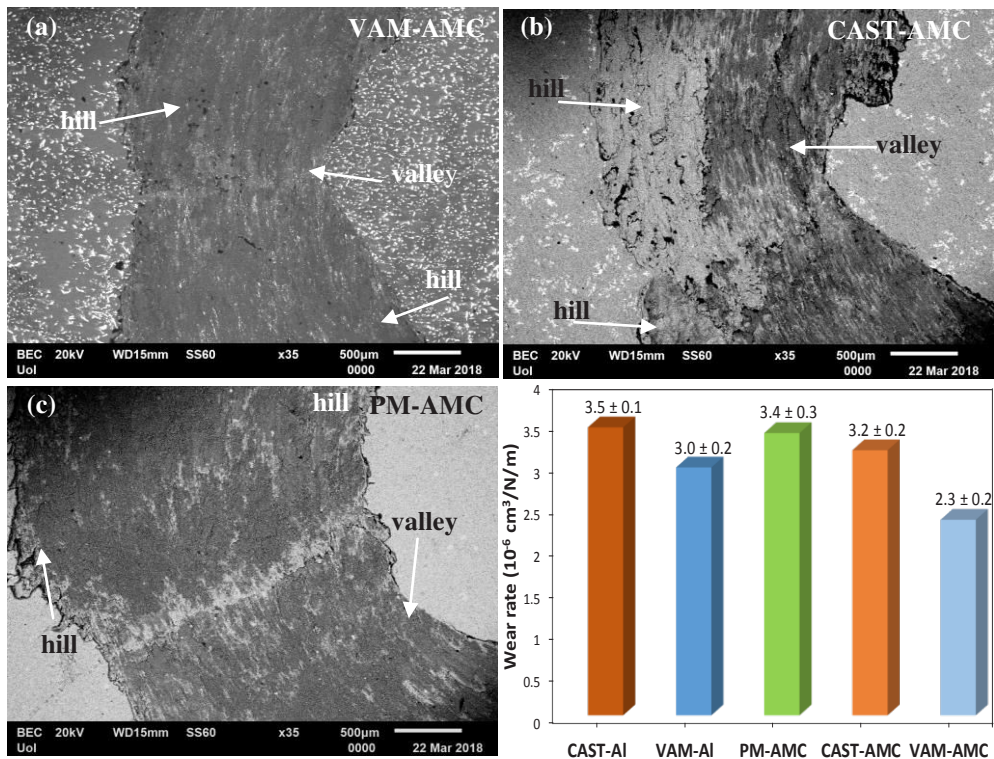


Fig. 4. (a-c) Wear tracks of AMCs in BEC mode; (d) wear rates of AMCs and monolithic Al.

Interfacial cracking (Fig. 5) is the main form of cracking in VAM-AMC owing to the high surface area of Al/aluminide interfaces. Interfaces are common sites of crack initiation because the oxide layer is finer and less cohesive there. Fig. 5a indicates an important aspect of the role of an array of Al_xW particles on the wear mechanism of VAM-AMC: cracks have stopped or been deflected or notably weakened when running into Al_xW particles. Fig. 5b indicates another important aspect of the role of an array of Al_xW particles (Fig. 5c) on the wear mechanism of the VAM-AMCs: As the counter-ball ran into an interfacial crack, it caused uplifting of the material in front of the crack. However, full delamination of the uplifted material did not occur, possibly due to the load transfer from the soft matrix to the hard IMCps. This material uplifting obstructed the sliding movement of the counter-ball. When the crack traversed an area of Al-matrix poor in W (Fig. 5c), delamination occurred leading to a crater of rough interior.

On the above basis, a wear mechanism can be formulated: (a) At the onset of the wear test, the Al-matrix near the interfaces was subjected to intensive plastic deformation in front of the counter-body. As the test proceeded, notable material flow led to the periodic ‘‘hill-valley’’ morphology. The IMCps limited matrix flow resulting in smoother wear surfaces. Dry sliding-due frictional heating caused the formation of surface alumina-based layers. (b) Cracks were generated in the oxide layer (both on the Al-matrix and at the interfaces) due to frictional forces, the brittleness of the alumina-based surface layer and wear fatigue. Interfacial cracking was the main form of cracking in VAM-AMC owing to the large surface area of IMC/Al interfaces. (c) As the counter-ball ran into an interfacial crack, it

caused uplifting of the material in front of the crack. This partial delamination/material uplifting would obstruct/retard the sliding movement of the ball.

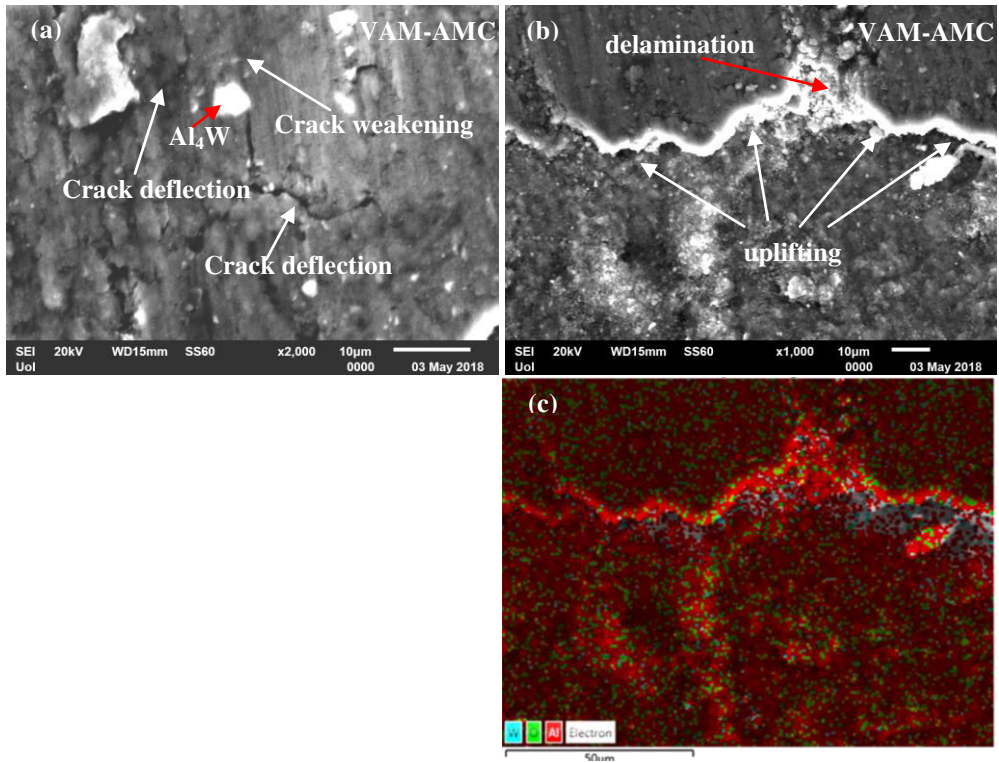


Fig. 5. VAM-AMC wear surfaces: (a) crack deflection/weakening, (b) material uplifting, (c) EDX map of (b) showing a crack propagated along an array of Al-W IMCps and delamination in an aluminide pure area (light-blue: W, green: O, red: Al).

4 Conclusions

Aluminium matrix composites (AMCs) fabricated by vacuum arc melting (VAM), stir casting (CAST) and free sintering (PM) were reinforced by several types of intermetallic particles (IMCps). The IMC nature (Al_4W (VAM, PM), Al_5W (VAM, PM), $Al_{12}W$ (PM) and $Al_3(Ti,W)$ (CAST)) and distribution strongly depends on the fabrication route. VAM-AMC presents the most uniform particle distribution, highest hardness and lowest porosity. The IMCp in-situ reinforcement improves the sliding wear response of Al. The “hill-valley” morphology of the wear tracks, reveals retention of the metallic nature of the AMCs. VAM-AMC shows the highest wear resistance, mainly attributed to the combination of low porosity, high hardness and uniform dispersion of IMCps. The proposed wear mechanism considers the “hill-valley” formation, the generation of cracks on the alumina-based surface layer both on the Al-matrix and at the different phase interfaces and the delaying role of the IMCps through crack deflection/weakening and material uplifting.

References

1. A. K. Chaubey, R. Kumar, T. Sahoo, IOP Conf. Ser.-Mat. Sci. **75**, 012011 (2015)

2. Y. Xue, R. Shen, S. Ni, M. Song, D. Xiao, J. Alloy Compd. **618**, 537 (2015)
3. H.B. Lee, H. Tezuka, E. Kobayashi, T. Sato, K.D. Woo, Mater. Trans. **53**, 428 (2012)
4. S. Scudino, G. Liu, M. Sakaliyska, J. Eckert, Acta Mater. **57**, 4529 (2009)
5. H. Zhang, P. Feng, F. Akhtar, Sci. Rep.-UK **7**, 12391 (2017)
6. A. Lekatou, A. Sfikas, A.E. Karantzalis, D. Sioulas, Corros. Sci. **63**, 193 (2012)
7. A. Lekatou, A.E. Karantzalis, A. Evangelou, V. Gousia, G. Kaptay, Z. Gacsi, P. Baumli, A. Simon, Mater. Des. **65**, 1121 (2015)
8. A. Lekatou, A.K. Sfikas, C. Petsa, A.E. Karantzalis, Metals **6** (2016) doi:10.3390/met6030046
9. A.G. Lekatou, A.K. Sfikas, A.E. Karantzalis, Mater. Chem. Phys. **200**, 33 (2017)
10. A.G. Lekatou, N. Gkikas, A.E. Karantzalis, G. Kaptay, Z. Gacsi, P. Baumli, A. Simon, Arch. Metall. Mater. **62**, 1235 (2017)
11. A.G. Lekatou, N. Gkikas, V. Gousia, A.E. Karantzalis, K. Lentzaris, J. Mater. Eng. Perform. (2018) (in press)
12. N. Stoloff, C. Liu, S. Deevi, Intermetallics **8**, 1313 (2000)
13. A. Evirgen, M. Lutfi Ovecoglu, J Alloy Compd. **496**, 212 (2010)
14. R.S. Rajamure, H.D. Vora, S.G. Srinivasan, N.B. Dahotre, Appl. Surf. Sci. **328**, 205, (2015)
15. J.M. Wu, Z.Z. Li, Wear **244**, 147 (2000)
16. A.A. Hamid, P.K. Ghosh, S.C. Jain, S. Ray, Wear **265**, 14 (2008)
17. S. Kumar, M. Chakraborty, V.S. Sarma, B.S. Murty, Wear **265**, 134 (2008)
18. S. Koksai, F. Ficici, R. Kayikci, O. Savas, Mater. Des. **42**, 124 (2012)
19. G. Gautam, N. Kumar, A. Mohan, R.K. Gautam, S. Mohan, Tribol. Int. **97**, 49 (2016)
20. N. Kumar, G. Gautam, R.K. Gautam, A. Mohan, S. Mohan, Tribol. Int. **97**, 313 (2016)
21. N.V. Rengasamy, M. Rajkumar, S.S. Kumaran, J. Alloy Compd. **658**, 757 (2016)
22. R. Varin, Metall. Mater. Trans. A **33**, 193 (2002)
23. R.H. Davies, A.T. Dinsdale, J.A. Gisby, J.A.J. Robinson, S.M. Martin, CALPHAD **26**, 229 (2002)
24. R.S. Rajamure, PhD Thesis, Univ. North Texas (2014)
25. N. El-Mahallawy, M.A Taha, A.E.W. Jarfors, H. Fredrikson, J Alloy Compd. **292**, 221 (1999)
26. T. Chen, M. Gao, Y.Tong, Metals **11**, 138 (2018)
27. M. Jahnatek, M. Krajei, J. Hafner, Phys. Rev. B **71**, 024101 (2005)
28. P. Villars (Chief Ed.), PAULING FILE in: Inorganic Solid Phases, Springer Materials (online database), (Springer-Verlag GmbH, 2016)
29. S. Knippscheer, G. Frommeyer, in Handbook of Aluminum: Vol. 2: Alloy Production and Materials Manufacturing, 603 (2003)
30. V.A. Chianeh, H.R.M. Hosseini, M. Nofar, J. Alloys Compd. **473**, 127 (2009)
31. C.A.C. Sequeira, L. Amaral, Trans. Nonferrous Met. Soc. China **24**, 1 (2014)
32. H.K.D.H. Bhadeshia, The Kirkendall Effect, Univ. Cambridge UK (web source) <https://www.phase-trans.msm.cam.ac.uk/kirkendall.html>
33. E. Basiri Tochaee, H.R. Madaah Hosseini, S.M. Seyed Reihani, J. Alloy Compd. **681**, 12 (2016)
34. V. Gousia, A. Tsioukis, A. Lekatou, A.E. Karantzalis, J. Mater. Eng. Perform. **25**, 3107 (2016)
35. A. Mandal, B.S. Murty, M. Chakraborty, Wear **266**, 865 (2009)
36. A.D. Sarkar, Friction and Wear, Academic Press (1980)
37. A.G. Lekatou, A. Pouliia, H. Mavros, A.E. Karantzalis, J. Mater. Eng. Perform. (2018) <https://doi.org/10.1007/s11665-018-3213-1>
38. D. Zois, A. Lekatou, M. Vardavoulias, T. Vaimakis, A.E. Karantzalis, Surf. Coat. Technol. **206**, 1469 (2011)